Complexes of Hydroxyl and Hydroperoxyl Radical with Formaldehyde, Acetaldehyde, and Acetone

Simone Aloisio and Joseph S. Francisco*

Department of Chemistry and Department of Earth and Atmospheric Sciences, Purdue University, West Lafayette, Indiana 47907

Received: October 25, 1999; In Final Form: January 21, 2000

We have calculated structures and energetics of complexes of HO_x (OH and HO_2) with formaldehyde, acetaldehyde, and acetone. These open shell systems form more strongly bound complexes than their counterpart closed shell water complexes. Binding energies (D_o) for these complexes were as high as 8.9 kcal mol^{-1} ($HO_2-CH_3COCH_3$). The hydroperoxyl radical forms more strongly bound complexes than the hydroxyl radical. Likewise, for the organic molecules studied, the strength of binding energies is consistently acetone > acetaldehyde > formaldehyde. Vibrational frequencies are also calculated and some relationships between these and binding energies and geometries are discussed. These data may be useful when laboratory data is present for these complexes. Equilibrium constants for the formation of these complexes are also calculated. As a result of this, it is predicted that the strongest of these complexes, the hydroperoxyl radical−acetone complex, will exist in the atmosphere under certain conditions.

I. Introduction

Much research has been done examining hydrogen bonding by studying weakly bound complexes. Hydrogen bonding is a critical factor in determining the physical properties of many solvated molecules, most notably in aqueous systems.[1] Many of the studies examine complexes formed exclusively made up of closed shell molecules, such as studies of the water dimer.[2] Recent calculations[3−11] of the water dimer estimate its binding energy (D_e) to be between 4.5 and 5.0 kcal mol^{-1}. Because of its importance in many chemical and most biological processes, water complexes with other molecules have also been studied.

There has been some work[12−25] studying the hydrogen bonding between water and carbonyl-containing molecules. Carbonyl-containing compounds are interesting from the perspective that they are commonly found in many chemical systems, and they form hydrogen bonds of comparable strength to that of the water dimer. In a recent work[26] from this laboratory, we have examined the properties of water complexes with formaldehyde, acetaldehyde and acetone. In that work, we calculate binding energies (D_e) of 4.5, 5.4, and 5.8 kcal mol^{-1}, respectively, for those complexes. In the case of water−formaldehyde[27,28] and water−acetone,[20] these complexes have also been experimentally observed using matrix isolation infrared spectroscopy techniques.

Hydroxyl (OH) and hydroperoxyl (HO_2) radical are important molecules involved in atmospheric, combustion, and biological processes. These are open shell molecules that have both been found to form complexes with water that have larger binding energies than the water dimer.[29,30] It is known that the OH radical reacts with formaldehyde, acetaldehyde, and acetone.[31] In the case of acetaldehyde, there is evidence that this reaction proceeds via a complex.[43] The hydroperoxyl radical reaction with formaldehyde is also thought to involve a complex.[46−49] To the best of our knowledge, calculations on the structure of these complexes have not been performed.

The scope of this work is to examine the structure and energetics of the complexes formed between the HO_x radicals (OH and HO_2) and formaldehyde, acetaldehyde, and acetone. One question that we ask is, are these radical−molecule complexes bound more strongly than their corresponding water complexes? We also present the vibrational frequencies of the complexes, and their shifts from the modes present in their parent monomers. These data may assist in the detection of these complexes using infrared spectroscopy.

II. Computational Methods

All calculations were performed using the GAUSSIAN 94[32] suite of programs. Geometries were optimized using the Becke three-parameter hybrid functional combined with Lee, Yang, and Parr correlation [B3LYP][33] density functional theory method. This method has been shown to be effective at accurately predicting structure and energetics when larger basis sets are used.[34−36] Furthermore, in our previous study[26] involving complexes of these organic molecules and water, frequency shifts calculated compared favorably to experimental data.[20,27,28] Basis sets employed are the 6-31G(d), 6-311++G(d,p), 6-311++G(2d,2p), and 6-311++G(3df,3pd). Frequency calculations were also performed at this level of theory for most of the complexes. For the acetone complexes, the frequency calculations were performed up to the B3LYP/6-311++G(2d,-2p) level of theory. The zero-point energy calculated from frequencies estimated at this level of theory was used to calculate the D_o at the higher level of theory. Otherwise, zero-point energies were taken from the same level of theory for this calculation. Zero-point energies taken from these frequency calculations can be assumed to be an upper limit due to the anharmonic nature of the potential energy surface.[37]

III. Results and Discussion

A. The Hydroxyl Radical−Formaldehyde Complex. Formaldehyde is an important molecule involved in both atmospheric and combustion chemistry. Its reaction with hydroxyl radical,

10.1021/jp993789c CCC: $19.00
Published on Web 03/21/2000

$$OH + CH_2O \rightarrow H_2O + HCO \quad (1)$$

is an important step in the oxidation of formaldehyde in the atmosphere and has been widely studied.[38−40] Here, we investigate the possibility of the formation of an adduct complex between OH and CH_2O, via the following reaction.

$$OH + CH_2O \rightarrow HO-CH_2O \quad (2)$$

Cheung and Li[41] calculate the structure of such a complex at the MP2/6-31G(d) level of theory, and the energetics of the complex using the G2 theoretical procedure. We compare our results to the ones obtained in that study.

The $HO-CH_2O$ complex is shown in Figure 1. The molecule is calculated to be planer at all levels of theory. The hydrogen atom of hydroxyl radical (H3) and the oxygen atom of formaldehyde (O1) bind the OH and CH_2O. There is a five membered ringlike structure formed between these molecules involving the H_1-C-O_1 of formaldehyde and the hydroxyl radical. The coordinates for the optimized structure at all levels of theory used in this study are given in Table 1. The intermolecular bond distance R1 for $HO-CH_2O$ is 1.965 Å at the B3LYP/6-311++G(3df,3pd) level of theory. Cheung and Li's structure,[41] which has the same connectivity and orientation as the one we calculate, calculate this distance to be 1.977 Å. We can compare this to the intermolecular bond distance that we have calculated for the complex between water and formaldehyde,[26] which is 1.976 Å at the same level of theory. The shorter bond distance in $HO-CH_2O$ indicates a slightly stronger bond. The $C-O_1$ bond distance in formaldehyde is calculated to be 1.202 Å at the highest level of theory. This is 0.3% longer than that in isolated CH_2O. This elongation is similar to the same elongation seen in the H_2O-CH_2O complex, which is 0.5%. The O_2-H_3 bond distance in the hydroxyl radical is 0.982 Å. This is 0.8% longer than that in isolated OH radical. This is identical to elongation of the analogous O−H bond in the H_2O-CH_2O complex. The H_1-C-O_1 bond angle, which makes part of the ring in the complex, is calculated to be 122.0°. This is similar, but not identical to the H_2-C-O_1 bond angle, which is 121.4°. The differing value of the in-ring angle indicates a perturbation caused by the hydroxyl radical, which makes part of the ring in the $HO-CH_2O$ complex. Cheung and Li,[41] who calculate 121.6° and 121.3° for the in-ring and out-of-ring H−C−O bond angles respectively, observe the same phenomenon. This is also seen in the complex between water and formaldehyde, which have in and out-of ring H−C−O bond angles of 121.3° and 121.7°. The intermolecular $O_1-H_3-O_2$ bond angle in $HO-CH_2O$ is calculated to be 172.7° at the highest level of theory. Cheung and Li[41] calculate a much smaller O−H−O angle of 152.1°. Using the same basis set as those authors, we also calculated a smaller bond angle, 166.2°. We feel that the 6-31G(d) basis probably overestimates the interaction between the hydrogen atom on formaldehyde, H_1, and the oxygen atom on the hydroxyl radical, O_2, which causes the calculated O−H−O bond angle to be smaller than it actually is. For H_2O-CH_2O, this basis set effect is also seen, with the O−H−O bond angle being calculated to be 147.4° using the 6-31G(d) basis set and 154.6° using the 6-311++G(3df,3pd) basis set. R2 is the distance between the oxygen atom in OH, O_3, and the nearest hydrogen atom in CH_2O, H_1. At the highest level of theory, this distance is 3.721 Å. The smaller O−H−O bond angle in H_2O-CH_2O results in a shorter R2, 2.909 Å at the same level of theory. The shorter distance in H_2O-CH_2O implies a possibly stronger interaction in that coordinate than for $HO-CH_2O$.

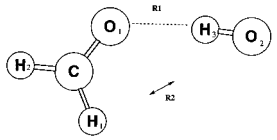

Figure 1. The hydroxyl radical−formaldehyde complex.

TABLE 1: Geometry of the Hydroxyl Radical−Formaldehyde Complex[a]

	B3LYP			
coordinate	6-31G(d)	6-311++ G(d,p)	6-311++ G(2d,2p)	6-311++ G(3df,3pd)
R1	1.950	1.956	1.951	1.965
R2	3.341	3.869	3.712	3.721
H_1C	1.107	1.106	1.103	1.103
H_1C	1.106	1.105	1.102	1.103
CO_1	1.211	1.205	1.204	1.202
O_2H_3	0.989	0.982	0.982	0.982
H_1CO_1	122.3	122.0	121.9	122.0
H_2CO_1	121.5	121.4	121.3	121.4
CO_1H_3	144.8	131.3	125.8	126.3
$O_1H_3O_2$	166.3	172.4	172.3	172.7
$H_1CO_1H_3$	0.0	0.0	0.0	0.0
$H_2CO_1H_3$	180.0	180	180.0	180.0
$CO_1H_3O_2$	0.0	0.0	0.0	0.0

[a] Bond distances are given in Ångstroms, bond angles in degrees.

TABLE 2: Rotational Constants for the Complexes[a]

		B3LYP			
molecule	constant	6-31G(d)	6-311++ G(d,p)	6-311++ G(2d,2p)	6-311++ G(3df,3pd)
$HO-CH_2O$	*A*	50391	74394	65586	66792
	B	4920	4010	4150	4163
	C	4148	3805	3903	3919
$HO-CH_3CHO$	*A*	35558	49803	45656	46224
	B	2344	2161	2216	2221
	C	2229	2098	2141	2147
$HO-CH_3COCH_3$	*A*	9209	8978	9067	9085
	B	2322	2117	2163	2170
	C	1898	1750	1785	1790
HO_2-CH_2O	*A*	18592	19250	19194	19356
	B	3644	3488	3497	3496
	C	3047	2953	2958	2961
HO_2-CH_3CHO	*A*	14108	15222	14998	15151
	B	1877	1792	1805	1802
	C	1673	1619	1627	1627
$HO_2-CH_3COCH_3$	*A*	7303	7297	7337	7363
	B	1495	1482	1489	1493
	C	1260	1251	1257	1260

[a] All rotational constants are reported in MHz.

The rotational constants for $HO-CH_2O$ are listed in Table 2. They are calculated to be 66792, 4163, and 3919 MHz at the B3LYP/6-311++G(3df,3pd) level of theory. The molecule is an asymmetric rotor. This can be seen in the structure shown in Figure 1. However, $A > B \approx C$, indicating that the molecule is a near-oblate top. This is similar to H_2O-CH_2O, which has rotational constants of 42115, 4727, and 4251 MHz at the same level of theory.

The hydroxyl radical−formaldehyde complex has 12 fundamental modes. Six of these modes are similar to the parent monomer formaldehyde, and one is similar to the hydroxyl radical vibrational mode. The remaining five modes are intermolecular and unique to the complex. The shifts in the modes in common with the parent monomer modes indicate how much the two monomers affect each other in complex form. More strongly bound complexes will have modes that are shifted by a larger amount than more weakly bound complexes. The vibrational modes for the $HO-CH_2O$ complex, including the

TABLE 3: Vibrational Frequencies of the Hydroxyl Radical−Formaldehyde Complex[a]

		B3LYP/6-311++G(3df,3pd)		
mode number	mode description	frequency	intensity	shift
1	hydroxyl O−H stretch	3571	344.7	−141
2	CH_2O C−H_2 asymmetric stretch	2991	74.4	+47
3	CH_2O C−H_2 symmetric stretch	2918	66.6	+32
4	CH_2O C−O stretch	1810	136.7	−11
5	CH_2O H−C−H bend	1533	16.9	+2
6	CH_2O H−C−O bend	1270	10.4	+5
7	CH_2O torsion	1208	5.8	+8
8	H_3-O_1 stretch	561	96.0	
9	$O_1-H_3-O_2$ bend	439	125.1	
10	intermolecular torsion	176	14.6	
11	intermolecular torsion	139	0.8	
12	$C-O_1-H_3$ bend	55	8.9	

[a] Frequencies and shifts are given in cm^{-1}; intensities are given in km mol^{-1}.

shifts relative to the similar modes of the parent monomers, the intensities of these bands, and the description of the modes; are listed in Table 3. The most shifted mode is the O−H stretch in the hydroxyl radical (mode number 1), which is red shifted by 141 cm^{-1}. This is consistent with the elongation of the O−H bond length when complexed with formaldehyde. Likewise, the C−O stretch of formaldehyde (mode number 4) is red-shifted by 11 cm^{-1} with respect to isolated CH_2O. In the water−formaldehyde complex,[26] this mode is red-shifted by 16 cm^{-1}, indicating a stronger intermolecular bond in the case of H_2O-CH_2O. The C−H_2 asymmetric and symmetric stretch modes (modes 2 and 3) are both blue-shifted 47 and 32 cm^{-1}, respectively, in the hydroxyl radical−formaldehyde complex. The corresponding shifts in the water−formaldehyde complex are 51 and 32 cm^{-1}. The most intense bands in the complex are the hydroxyl radical O−H stretch (mode 1) at 3571 cm^{-1}, the CH_2O C−O stretch (mode 4) at 1810 cm^{-1}, the intermolecular O−H stretch (mode 8) at 561 cm^{-1}, and the intermolecular O−H−O bend (mode 9) at 439 cm^{-1}. Of these, the two intramolecular bands are significantly shifted, while the two intermolecular bands are in the mid-IR. Because of this, these bands should be the most likely to be observed in experiments. The analogous intermolecular O−H stretch frequency of H_2O-CH_2O is calculated to be 531 cm^{-1}.

B. Hydroxyl Radical−Acetaldehyde Complex. The reaction of hydroxyl radical with acetaldehyde:

$$OH + CH_3CHO \rightarrow CH_3CO + H_2O \qquad (3)$$

is another important reaction involved in the oxidation of hydrocarbons in both combustion and atmospheric chemistry. It is thought to be the major sink for acetaldehyde in the atmosphere. Furthermore, this reaction has been found to exhibit a negative temperature dependence.[42−44] Michael et al.[43] attribute this negative temperature dependence to the formation of an adduct being formed. The adduct formed, the hydroxyl radical−acetaldehyde complex, is formed by the following reaction.

$$OH + CH_3CHO \rightarrow HO-CH_3CHO \qquad (4)$$

The $HO-CH_3CHO$ complex is the focus of this section of our study.

The structure of the hydroxyl radical−acetaldehyde complex is shown in Figure 2. As is the case for $HO-CH_2O$, the intermolecular bond is between the hydrogen atom on the OH, H_5, and the oxygen atom of acetaldehyde, O_1. The hydroxyl radical and the H_1,C, and O_1 atoms of acetaldehyde form a five-membered [a]Relative energies are [a]Relative energies are structure, similar to the one formed by the hydroxyl radical−formaldehyde complex. In a previous work, we have also calculated the structure of the water−acetaldehyde complex.[26] It is interesting to note that in the H_2O-CH_3CHO complex, the lowest energy structure is that in which the oxygen on the water molecule oriented so that is it closer to the methyl group in acetaldehyde. However, for the hydroxyl radical−acetaldehyde complex, this was not found to be the case. The coordinates for the geometry of the hydroxyl radical−acetaldehyde complex are listed in Table 4. The hydroxyl radical−acetaldehyde complex has an intermolecular bond distance, R1, of 1.899 Å at the B3LYP/6-311++G(3df,3pd) level of theory. This is 0.066 Å shorter than the intermolecular bond distance in $HO-CH_2O$, indicating a stronger bond. This is also shorter than the intermolecular bond distance in the water-acetaldehyde complex, which is calculated to be 1.942 Å at the same level of theory. The carbon−oxygen bond in acetaldehyde, C_1-O_1 is elongated by 0.4% in the complex with respect to isolated acetaldehyde, with a calculated value of 1.208 Å. This is similar in magnitude to the elongation of the C−O bond in $HO-CH_2O$, and identical to the calculated C_1-O_1 bond distance in H_2O-CH_3CHO. The oxygen−hydrogen bond distance of the hydroxyl radical, O_2-H_5, is 0.983 Å. This is 0.9% longer than in isolated OH, only slightly more elongated than in $HO-CH_2O$. This is the same magnitude of elongation as seen in the analogous oxygen−hydrogen bond in the water of H_2O-CH_3CHO. The H_1-C_1 bond distance in $HO-CH_3CHO$ is 1.107 Å, which is 0.3% shorter than in isolated acetaldehyde. The $H_1-C_1-O_1$ bond angle in $HO-CH_3CHO$ is 120.0°, only 0.2% less than in isolated CH_3CHO. Interestingly, the $C_2-C_1-O_1$ bond angle is 0.3% less

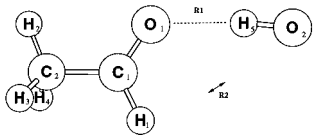

Figure 2. The hydroxyl radical−acetaldehyde complex.

TABLE 4: Geometry of the Hydroxyl Radical−Acetaldehyde Complex[a]

	B3LYP			
coordinate	6-31G(d)	6-311++G(d,p)	6-311++G(2d,2p)	6-311++G(3df,3pd)
R1	1.918	1.925	1.910	1.899
R2	3.305	3.769	3.598	3.628
C_1O_1	1.216	1.205	1.210	1.208
C_1H_1	1.110	1.109	1.068	1.107
C_1C_2	1.502	1.498	1.496	1.495
C_2H_2	1.092	1.089	1.087	1.087
C_2H_3	1.098	1.096	1.093	1.093
C_2H_4	1.098	1.096	1.093	1.093
O_2H_5	0.990	0.984	0.989	0.983
$H_1C_1O_1$	120.2	120.4	118.8	120.0
$C_2C_1O_1$	124.1	123.9	124.2	124.4
$H_2C_2C_1$	110.7	111.1	111.1	111.2
$H_3C_2C_1$	109.6	109.3	109.3	109.2
$H_4C_2C_1$	109.6	109.3	109.3	109.2
$C_1O_1H_5$	115.0	129.2	124.5	124.9
$O_1H_5O_2$	167.9	173.5	173.3	173.9
$H_2C_2C_1O_1$	0.0	0.0	0.0	0.0
$H_3C_2C_1O_1$	121.7	121.9	121.9	122.0
$H_4C_2C_1O_1$	−121.7	−121.9	−121.9	−122.0
$H_1C_1O_1H_5$	0.0	0.0	0.0	0.0
$C_1O_1H_5O_2$	0.0	0.0	0.0	0.0

[a] Bond distances are given in Ångstroms, bond angles in degrees.

TABLE 5: Vibrational Frequencies of the Hydroxyl Radical−Acetaldehyde Complex[a]

		B3LYP/6-311++G(3df,3pd)		
mode number	mode description	frequency	intensity	shift
1	hydroxyl O−H stretch	3532	476.7	−180
2	CH_3CHO sp^3 C−H stretch	3144	5.9	+56
3	CH_3CHO sp^3 C−H stretch	3077	3.1	+2
4	CH_3CHO sp^3 C−H stretch	3025	1.3	+2
5	CH_3CHO sp^2 C−H stretch	2914	75.3	+41
6	CH_3CHO C−O stretch	1797	254.7	−16
7	CH_3CHO sp^3 torsion	1467	10.9	−2
8	CH_3CHO H−C−H bend	1459	27.0	−2
9	CH_3CHO H−C−O bend	1429	8.8	+7
10	CH_3CHO C−C stretch	1384	28.6	+3
11	CH_3CHO H−C−C bend	1141	0.3	+5
12	CH_3CHO H−C−C bend	1139	25.0	+9
13	CH_3CHO torsion	897	6.8	+11
14	CH_3CHO torsion	786	0.3	+7
15	H_5-O_1 stretch	595	93.0	
16	CH_3CHO torsion	528	27.2	+17
17	$O_1-H_5-O_2$ bend	467	119.4	
18	intermolecular torsion	165	7.5	
19	CH_3CHO CH_3 twist	161	0.4	+2
20	intermolecular torsion	54	0.6	
21	$C_1-O_1-H_5$ bend	41	2.9	

[a] Frequencies and shifts are given in cm^{-1}; intensities are given in km mol^{-1}.

in the complex than in isolated acetaldehyde. This effect is probably due to the difference in the C−O bond distances between the complex and the isolated monomer. The intermolecular $O_1-H_5-O_2$ bond angle is 173.9°. This is 1.2° more than in the hydroxyl radical−formaldehyde complex. However, the distance between the oxygen atom of the hydroxyl radical, O_2, and the in-ring hydrogen of the acetaldehyde, H_1 (R2) is calculated to be 3.628 Å. This is 0.093 Å shorter than R2 for $HO-CH_2O$. This is due to the decreased intermolecular bond distance R1 in the hydroxyl radical−acetaldehyde complex. The interaction between the two atoms in the R2 coordinate is similar for both $HO-CH_2O$ and $HO-CH_3CHO$.

The rotational constants for $HO-CH_3CHO$ at the B3LYP6-311++G(3df,3pd) level of theory are 46224, 2221, and 2147 MHz. The rotational constants at all the levels of theory employed in this study are listed in Table 2. The hydroxyl radical−acetaldehyde complex is an asymmetric rotor. This can be seen in the structure shown in Figure 2. However, $A > B \approx C$, indicating that the molecule is a near-oblate top. This is not the case for H_2O-CH_3CHO, which is clearly an asymmetric rotor.

The vibrational frequencies for the hydroxyl radical−acetaldehyde complex are given in Table 5. There are 21 fundamental vibrational frequencies; 15 from acetaldehyde, one from the hydroxyl radical, and five intermolecular modes. The hydroxyl radical O−H stretch mode (mode 1) is the most shifted from the same mode in isolated OH. It has a calculated frequency of 3532 cm^{-1}, 180 cm^{-1} lower in energy than the O−H stretch in isolated hydroxyl radical. This is 39 cm^{-1} more than in the $HO-CH_2O$ complex, reflecting a stronger interaction between OH and CH_3CHO. This is also the strongest absorbing band, with a calculated intensity of 476.7 km mol^{-1}. The C−O stretch (mode 6) in $HO-CH_3CHO$ is red-shifted by 16 cm^{-1}. This is a larger shift than in $HO-CH_2O$ (11 cm^{-1}), but not H_2O-CH_3CHO[26] (18 cm^{-1}). The altered geometry of the acetaldehyde in CH_3CHO causes mode numbers 2 (primarily the H_2-C_2 stretch) and 5 to be blue shifted by 56 and 41 cm^{-1}, respectively. An interaction along the R2 coordinate is not the likely source of these shifts due to the large distance between the oxygen atom of OH and the hydrogen atoms that are primarily involved in these vibrational motions. Similar shifts can be seen in H_2O-CH_3CHO, with magnitudes of 58 and 32 cm^{-1}, respectively. The intermolecular O−H stretching mode (mode 15) is located at 595 cm^{-1}. This is 34 cm^{-1} higher in energy than the analogous mode in $HO-CH_2O$ and 21 cm^{-1} higher in energy than the analogous mode in H_2O-CH_3CHO. On the basis of shifts from parent monomers and intensities, the most likely modes to be observed in experiments are modes 1, 5, 6, 15, and 16.

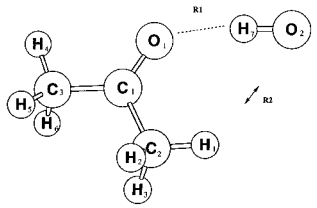

Figure 3. The hydroxyl radical−acetone complex.

C. Hydroxyl Radical−Acetone Complex. Acetone is another atmospherically important molecule that is oxidized by hydroxyl radical. It is curious that the reaction

$$OH + CH_3COCH_3 \rightarrow CH_3COCH_2 + H_2O \qquad (5)$$

shows a positive temperature dependence,[45] while reaction 3 shows a negative temperature dependence and reaction 1 shows no temperature dependence at all. This means that if the acetone-hydroxyl radical reaction does have an adduct forming channel, this channel is either negligible or a hindrance to the formation of the products for reaction 5. The reaction forming the hydroxyl radical−acetone complex is given below.

$$OH + CH_3COCH_3 \rightarrow HO-CH_3COCH_3 \qquad (6)$$

The structure of the hydroxyl radical−acetone complex is given in Figure 3. Like the $HO-CH_2O$ and $HO-CH_3CHO$ complexes discussed earlier, $HO-CH_3COCH_3$ has a ringlike structure. For the hydroxyl radical−acetone complex, this is a six-membered ring formed by the hydroxyl radical and H_1, C_2, C_1, and O_1 of the acetone molecule. The fully optimized geometry of $HO-CH_3COCH_3$ at all levels of theory used in this study is shown in Table 6. The intermolecular bond formed between the hydrogen atom of the hydroxyl radical and the oxygen atom of acetone R1 has a length of 1.869 Å at the B3LYP/6-311++G(3df,3pd) level of theory. This is 0.030 Å shorter than in $HO-CH_3CHO$ and 0.096 Å shorter than in $HO-CH_2O$, indicating that it is the strongest bond in this series of complexes. This is also true of the complex between water and acetone,[26] which has an intermolecular bond distance of 1.911 Å at the same level of theory. From this, we can conclude that the intermolecular bond in $HO-CH_3COCH_3$ is stronger than that in $H_2O-CH_3COCH_3$. The carbon−oxygen bond distance acetone, C_1-O_1, is 1.214 Å. This bond distance is elongated by 0.4% relative to isolated CH_3COCH_3, consistent with what we have calculated in the other complexes mentioned thus far. This elongation is identical to what is calculated for the water−acetone complex. The oxygen−hydrogen bond distance of the hydroxyl radical is 0.985 Å, which is 1.1% longer than that in isolated OH. This is consistent with the stronger intermolecular bond we have seen for this complex relative to the others in this study. It seems that, as the intermolecular bond becomes stronger for each of these complexes, it is the oxygen−hydrogen bond of OH that becomes weaker to a greater extent than the carbon−oxygen bond of the organic molecule. The carbon−carbon−oxygen bond angles in isolated acetone are identical

TABLE 6: Geometry of the Hydroxyl Radical−Acetone Complex[a]

	B3LYP			
coordinate	6-31G(d)	6-311++ G(d,p)	6-311++ G(2d,2p)	6-311++ G(3df,3pd)
R1	1.881	1.884	1.879	1.869
R2	2.467	3.118	2.958	2.972
C_1O_1	1.224	1.217	1.216	1.214
C_1C_2	1.515	1.513	1.510	1.509
C_1C_3	1.515	1.511	1.490	1.509
C_2H_1	1.092	1.089	1.086	1.087
C_2H_2	1.098	1.095	1.092	1.093
C_2H_3	1.097	1.093	1.092	1.091
C_3H_4	1.092	1.089	1.093	1.086
C_3H_5	1.097	1.094	1.099	1.091
C_3H_6	1.097	1.095	1.099	1.092
O_2H_7	0.993	0.986	0.985	0.985
$C_2C_1O_1$	122.1	121.9	121.9	121.9
$C_3C_1O_1$	120.6	121.0	120.9	121.1
$H_1C_2C_1$	110.3	110.7	110.8	110.9
$H_2C_2C_1$	109.8	109.0	109.7	109.2
$H_3C_2C_1$	110.4	110.9	110.2	110.7
$H_4C_3C_1$	110.1	110.3	111.2	110.4
$H_5C_3C_1$	110.5	110.8	111.4	110.5
$H_6C_3C_1$	110.0	109.3	110.7	109.5
$C_1O_1H_7$	116.7	130.7	127.0	127.2
$O_1H_7O_2$	165.3	170.5	171.0	171.2
$H_1C_2C_1O_1$	−3.3	−11.2	−2.4	−8.6
$H_2C_2C_1O_1$	117.6	108.7	118.6	111.7
$H_3C_2C_1O_1$	−125.1	−133.8	−124.1	−131.0
$H_4C_3C_1O_1$	−3.3	−8.3	−3.8	−5.7
$H_5C_3C_1O_1$	117.5	130.6	125.5	127.8
$H_6C_3C_1O_1$	−124.9	−111.9	−117.0	−114.9
$C_2C_1O_1H_7$	1.7	0.6	−0.3	0.8
$C_3C_1O_1H_7$	181.7	180.4	179.8	180.6
$C_1O_1H_7O_2$	2.0	0.1	8.3	−2.2

[a] Bond distances are given in Ångstroms, bond angles in degrees.

TABLE 7: Vibrational Frequencies of the Hydroxyl Radical−Acetone Complex[a]

		B3LYP/6-311++G(2d,2p)		
mode number	mode description	frequency	intensity	shift
1	hydroxyl O−H stretch	3509	485.1	−203
2	CH_3COCH_3 C−H stretch	3151	5.9	+5
3	CH_3COCH_3 C−H stretch	3146	7.1	+1
4	CH_3COCH_3 C−H stretch	3095	6.2	+5
5	CH_3COCH_3 C−H stretch	3087	6.2	+5
6	CH_3COCH_3 C−H stretch	3043	5.7	+3
7	CH_3COCH_3 C−H stretch	3036	0.1	+4
8	CH_3COCH_3 C−O stretch	1760	249.1	−19
9	CH_3COCH_3 C−C−H bend	1493	18.8	0
10	CH_3COCH_3 C−C−H bend	1477	34.8	+1
11	CH_3COCH_3 C−C−H bend	1470	3.9	0
12	CH_3COCH_3 C−C−H bend	1466	1.4	0
13	CH_3COCH_3 C−C−H bend	1400	46.8	+7
14	CH_3COCH_3 C−C−H bend	1397	30.0	+5
15	CH_3COCH_3 C−C−C asymmetric stretch	1251	65.0	+15
16	CH_3COCH_3 torsion	1125	3.4	+3
17	CH_3COCH_3 C−C−C symmetric stretch	1092	0.3	+2
18	CH_3COCH_3 C−C−O bend	899	7.3	+9
19	CH_3COCH_3 C−C−O bend	894	0.4	+6
20	CH_3COCH_3 torsion	792	0.9	+10
21	H_7-O_1 stretch	618	83.6	
22	CH_3COCH_3 torsion	552	25.4	+16
23	CH_3COCH_3 torsion	493	0.8	+2
24	$O_1-H_7-O_2$ bend	465	141.0	
25	CH_3COCH_3 torsion	388	3.3	+8
26	intermolecular torsion	169	7.5	
27	CH_3COCH_3 torsion	129	0.2	−1
28	intermolecular torsion	40	0.2	
29	$C-O_1-H_7$ bend	34	3.3	
30	CH_3COCH_3 torsion	32	0.2	+16

[a] Frequencies and shifts are given in cm^{-1}; intensities are given in km mol^{-1}.

to each other. In the hydroxyl radical−acetone complex, however, $C_2-C_1-O_1$, which is in the proximity of the hydroxyl radical, is 0.2% less; and $C_3-C_1-O_1$, which is one the other side of the hydroxyl radical, is 0.5% more than that in an isolated acetone molecule. This is similar to what is observed for $H_2O-CH_3COCH_3$, in which these angles are 0.3% less and 0.5% more than isolated acetone, respectively. The intermolecular $O_1-H_7-O_2$ bond angle is 171.2° in $HO-CH_3COCH_3$. This is slightly shorter than the analogous angle in either $HO-CH_2O$ or $HO-CH_3CHO$. Again, this is a larger angle than that seen in the complex of water and acetone, which has an corresponding value of 165.9° at the same level of theory. The intermolecular distance between O_2 and H_1, R2, is 2.972 Å. This is shorter than that for either the hydroxyl radical−formaldehyde or the hydroxyl radical−acetaldehyde complexes. This is 0.374 Å shorter than the analogous distance in the water−acetone complex. This is consistent with what is seen in the other hydroxyl radical complexes studied in this work and their corresponding molecules involving water.

The rotational constants for the hydroxyl radical−acetone complex are listed in Table 2. At the highest level of theory, B3LYP/6-311++G(3df,3pd), the rotational constants are 9085, 2170, and 1790 MHz. These constants are consistent with the structure shown in Figure 3. $HO-CH_3COCH_3$ is not a near-oblate top like the other hydroxyl radical complexes in this study. It has rotational constants similar to those for $H_2O-CH_3COCH_3$, which are 9172, 2162 and 1788 MHz at the same level of theory.

The hydroxyl radical−acetone complex has 30 fundamental vibrational frequencies. Of these, 24 are modes present in isolated acetone, one is present in the hydroxyl radical, and five are unique intermolecular modes. These vibrational frequencies, along with their intensities and shifts relative to the parent monomers, are listed in Table 7. Just as was the case for $HO-CH_2O$ and $HO-CH_3CHO$, the hydroxyl radical O−H stretch (mode number 1) is the most shifted mode. In the case of $HO-CH_3COCH_3$, this shift is 203 cm^{-1} to the red of isolated OH. This is larger than either of the other two hydroxyl radical complexes studied in this work, supporting the evidence that this is the most strongly bound complex of those three complexes. The C−O stretch (mode 8) of the acetone molecule is also red-shifted by 19 cm^{-1}. This is consistent with the elongation along this coordinate calculated in the structure of $HO-CH_3COCH_3$. This shift is larger than the analogous red-shift in this mode for $HO-CH_2O$ by 8 cm^{-1}, and $HO-CH_3CHO$ by 3 cm^{-1}. This is 1 cm^{-1} less than the red shift calculated[26] for $H_2O-CH_3COCH_3$, however. The intermolecular O−H stretch frequency (mode 21) for the hydroxyl radical−acetone complex is calculated to be 618 cm^{-1}. This is higher in energy than the similar intermolecular frequencies for the hydroxyl radical−acetone complex (561 cm^{-1}), and the water−acetone complex (593 cm^{-1}). Along with the three previously mentioned modes, the intermolecular $O_1-H_7-O_2$ bend is also an intense band for $HO-CH_3COCH_3$. It has a calculated intensity of 141.0 km mol^{-1}. The four fundamental bands of the hydroxyl radical−acetone complex discussed above are the most likely to be observed using infrared spectroscopy.

D. The Hydroperoxyl Radical−Formaldehyde Complex. Formaldehyde reacts with the hydroperoxyl radical much more slowly than it reacts with the hydroxyl radical.[31] There is sufficient evidence from experiments[46−49] which show that this reaction goes through an adduct HO_2-CH_2O complex, which

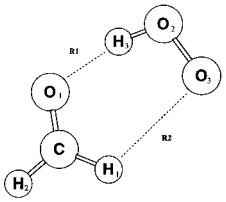

Figure 4. The hydroperoxyl radical−formaldehyde complex.

TABLE 8: Geometry of the Hydroperoxyl Radical−Formaldehyde Complex[a]

	B3LYP			
coordinate	6-31G(d)	6-311++ G(d,p)	6-311++ G(2d,2p)	6-311++ G(3df,3pd)
R1	1.801	1.798	1.785	1.777
R2	2.513	2.725	2.702	2.719
H_1C	1.102	1.102	1.099	1.100
H_2C	1.106	1.104	1.101	1.102
CO_1	1.216	1.210	1.209	1.206
H_3O_2	0.996	0.991	0.990	0.990
O_2O_3	1.333	1.329	1.330	1.325
H_1CO_1	121.6	121.4	121.4	121.5
H_2CO_1	120.7	120.8	120.6	120.8
$H_3O_2O_3$	103.6	104.3	104.0	104.1
CO_1H_3	113.2	119.1	116.8	117.3
$O_1H_3O_2$	161.8	161.9	164.5	164.7
$H_1CO_1H_3$	0.0	0.0	0.0	0.0
$H_2CO_1H_3$	180.0	180.0	180.0	180.0
$CO_1H_3O_2$	0.0	0.0	0.0	0.0
$O_1H_3O_2O_3$	0.0	0.0	0.0	0.0

[a] Bond distances are given in Ångstroms, bond angles in degrees.

rapidly rearranges to form a organic peroxy radical as shown in the reaction below.

$$HO_2 + CH_2O \rightarrow HO_2{-}CH_2O \rightarrow HOCH_2O_2 \qquad (7)$$

In this section, we investigate the properties of the hydroperoxyl radical−formaldehyde complex.

The structure of the hydroperoxyl radical−formaldehyde complex is shown in Figure 4. The molecule is planer, with the intermolecular bond R1 between the oxygen atom of formaldehyde and the hydrogen atom of the hydroperoxyl radical. The $HO_2{-}CH_2O$ complex has a six-membered ring like structure, with the HO_2 radical forming part of the ring, and all the atoms of formaldehyde except one of the hydrogens forming the rest of the ring. The fully optimized coordinates are given in Table 8 for all the levels of theory used in this study. At the B3LYP/6-311++G(3df,3pd) level of theory, the highest used in this study, the intermolecular bond distance R1 is calculated to be 1.777 Å. This is 0.188 Å shorter than the intermolecular bond distance for the hydroxyl radical−formaldehyde complex, and 0.199 Å shorter than the water−formaldehyde complex.[26] This represents a 10.6% decrease in R1 compared to $HO{-}CH_2O$ and an 11.2% decrease in R1 compared to $H_2O{-}CH_2O$, indicating a significantly stronger bond in $HO_2{-}CH_2O$ than these two complexes. As a result of this, the hydrogen−oxygen bond distance in the hydroperoxyl radical is elongated by 1.5% to 0.990 Å in the complex with respect to isolated HO_2. This is larger than the elongation of the analogous hydrogen−oxygen bonds in either $HO{-}CH_2O$ (0.8%) or $H_2O{-}CH_2O$ (0.8%). The elongation of the carbon−oxygen bond in formaldehyde is also larger, 0.7% compared to 0.3% for $HO{-}CH_2O$ and 0.5% for $H_2O{-}CH_2O$. As was the case for both the hydroxyl radical−formaldehyde complex and the water formaldehyde complex, the H−C−O angles on the formaldehyde are not equal in the hydroperoxyl radical−formaldehyde complex. In this case, the $H_1{-}C{-}O_1$ angle is 121.5°, while the $H_2{-}C{-}O_1$ complex is 120.8°. These are less than the H−C−O angle in isolated formaldehyde by 0.4% and 1.1% respectively. The elongation of the carbon−oxygen bond can explain the shortening of the bond angle. The fact that the angles are not equal to each other is evidence that there is an interaction between the HO_2 terminal oxygen and H_1 from formaldehyde. This interaction causes the in-ring formaldehyde H−C−O bond angle to by 0.7° larger than the out-of-ring H−C−O bond angle. The hydroperoxyl bond angle is 1.2% shorter in the $HO_2{-}CH_2O$ complex than in isolated HO_2. This is also evidence for a second interaction between the two monomers when complexed. The distance between the terminal oxygen in HO_2 and the in-ring hydrogen of formaldehyde in $HO_2{-}CH_2O$ is calculated to be 2.719 Å at the highest level of theory. This is 37% less than the comparable difference in $HO{-}CH_2O$ and 7% less than in $H_2O{-}CH_2O$. One would expect this to translate to a much stronger interaction between these two atoms in the case of $HO_2{-}CH_2O$, which appears to be the case.

TABLE 9: Vibrational Frequencies of the Hydroperoxyl Radical−Formaldehyde Complex[a]

		B3LYP/6-311++G(3df,3pd)		
mode number	mode description	frequency	intensity	shift
1	hydroperoxyl H−O stretch	3343	682.5	−259
2	CH_2O C−H_2 asymmetric stretch	3031	33.3	+87
3	CH_2O C−H_2 symmetric stretch	2937	76.5	+51
4	CH_2O C−O stretch	1790	106.4	−31
5	hydroperoxyl H−O−O bend	1555	58.4	+119
6	CH_2O H−C−H bend	1524	31.9	+7
7	CH_2O H−C−O bend	1274	7.9	+9
8	CH_2O torsion	1220	5.9	+20
9	hydroperoxyl O−O stretch	1197	18.6	+28
10	$H_3{-}O_1$ stretch	658	109.9	
11	$O_1{-}H_3{-}O_2$ bend	244	46.8	
12	intermolecular torsion	190	7.1	
13	intermolecular torsion	169	0.5	
14	$C{-}O_1{-}H_3$ bend	103	14.8	
15	intermolecular torsion	67	10.5	

[a] Frequencies and shifts are given in cm^{-1}; intensities are given in km mol^{-1}.

The rotational constants for the hydroperoxyl radical−formaldehyde complex are calculated to be 19356, 3496, and 2961 MHz at the B3LYP/6-311++G(3df,3pd) level of theory. $HO_2{-}CH_2O$ is an asymmetric rotor since $A \neq B \neq C$. This is consistent with the structure of the molecule shown in Figure 4.

There are 15 fundamental normal modes for the hydroperoxyl radical−formaldehyde complex. These vibrational frequencies are listed in Table 9. Of these modes, six are similar to modes in isolated formaldehyde, three are similar to modes in the hydroperoxyl radical, and the remaining six modes are unique to the complex. As in the complexes involving the hydroxyl radical in this study, and the complexes involving water in our previous study,[26] the hydrogen atom−oxygen atom stretch of the electron acceptor is the most shifted mode from the parent monomer frequency. In the case of $HO_2{-}CH_2O$, the O−H stretch of the hydroperoxyl radical (mode number 1) is calculated to have a vibrational frequency 259 cm^{-1} lower in

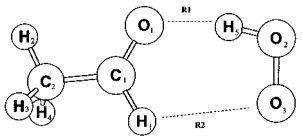

Figure 5. The hydroperoxyl radical−acetaldehyde complex.

energy than that of the isolated parent HO_2. This is somewhat analogous to the O−H stretch of the hydroxyl radical in HO−CH_2O, which is red-shifted 141 cm^{-1} with respect to its parent monomer OH. The H−O−O bend of the hydroperoxyl radical (mode 5) is the next most shifted mode in HO_2−CH_2O, with a calculated blue shift of 119 cm^{-1}. This is consistent with the structural change in the H−O−O angle, which is 1.2% less in the complex than that in isolated HO_2. The hydroperoxyl O−O stretch (mode 9) is shifted by 29 cm^{-1} to the blue of that mode in isolated HO_2. The C−O stretch of formaldehyde (mode 4) is red-shifted by 31 cm^{-1}. This same red shift is seen in HO−CH_2O and H_2O−CH_2O. In those molecules, the magnitude of the shift is smaller, 11 and 16 cm^{-1}, respectively. The larger shift in HO_2−CH_2O is reflective of the stronger bond formed between the hydroperoxyl radical and formaldehyde than in the case of the other two complexes. As was the case for the two other complexes, the H−C−H asymmetric (mode 2) and symmetric (mode 3) are blue shifted with respect to those of isolated formaldehyde. For HO_2−CH_2O, these shifts are 87 and 51 cm^{-1}, respectively. Theses shifts are 40 and 19 cm^{-1} larger than those seen in HO−CH_2O and 36 cm^{-1} and 19 cm^{-1} larger than those seen in H_2O−CH_2O, further showing the strength of the interaction between HO_2 and CH_2O. The intermolecular O_1−H_3 stretching frequency for the hydroperoxyl radical−formaldehyde complex (mode 10) is calculated to be 658 cm^{-1}. The corresponding frequencies for HO−CH_2O and H_2O−CH_2O are 561 and 531 cm^{-1}, respectively. The higher energy vibration of the HO_2−CH_2O complex is reflective of the shorter intermolecular bond distance of that molecule, and hence of the more strongly bound complex. The most intense bands of the HO_2−CH_2O complex are the hydroperoxyl radical O−H stretch (mode 1), the intermolecular O_1−H_3 stretch (mode 10), and the C−O stretch of formaldehyde (mode 4), which have calculated band strengths of 682.5, 109.9 and 106.4 km mol^{-1} respectively.

E. Hydroperoxyl Radical−Acetaldehyde Complex. Reaction of acetaldehyde and other higher aldehydes with the hydroperoxyl radical are known to be relatively slow at room temperature.[50] However, it is still possible for HO_2 and CH_3-CHO to form an adduct complex similar to the one that HO_2 forms with CH_2O.

$$HO_2 + CH_3CHO \rightarrow HO_2{-}CH_3CHO \qquad (8)$$

Whether this complex reacts further to form products is beyond the scope of this work; however, valuable information about the complex can be extracted which would be useful in making this type of prediction from the data that follows.

The hydroperoxyl radical−acetaldehyde complex is shown in Figure 5. Like the HO_2−CH_2O complex, the molecule forms a six-membered ring, with the primary intermolecular interaction occurring between the hydrogen of the HO_2 and the oxygen of the CH_3CHO. Like the hydroxyl radical−acetaldehyde complex, the ring is formed opposite the methyl group of acetaldehyde. The optimized geometries for the hydroperoxyl−acetaldehyde complex at all levels of theory used are listed in Table 10. The intermolecular bond distance R1 for the hydroperoxyl radical−acetaldehyde complex is 1.734 Å at the highest level of theory used, B3LYP/6-311++G(3df,3pd). This is shorter than the HO_2−CH_2O complex by 0.043 Å, indicating a stronger bond. It is also shorter than the comparable bonds for both the hydroxyl radical−acetaldehyde by 0.165 Å and water−acetaldehyde by 0.208 Å. The hydrogen−oxygen bond of the hydroperoxyl radical, H_5−O_2, is elongated by 1.8% to 0.993 Å. The carbon−oxygen bond distance is elongated by 0.8%. These are both manifestations of the stronger intermolecular bond of HO_2−CH_3CHO than either HO−CH_3CHO or H_2O−CH_3CHO. The H_1−C_1−O_1 bond angle is decreased by 0.6% relative to isolated acetaldehyde, while the C_2−C_1−O_1 bond angle is decreased by 0.8%. This is the same effect that is seen in the hydroxyl-radical acetaldehyde complex and is probably due to the elongation of the C_1−O_1 bond. The H_5−O_2−O_3 bond angle is decreased by 1.1% relative to isolated HO_2. As was the case for the hydroperoxyl radical−formaldehyde complex, this is evidence for a second intermolecular interaction between the terminal oxygen of HO_2 and the in-ring hydrogen of CH_3-CHO. The distance between these atoms R2 is 2.736 Å. This is longer than for HO_2−CH_2O, indicating that, if a interaction exists, it is a weaker one. The fact that the H_5−O_2−O_3 bond angle is slightly less decreased than in the hydroperoxyl radical−acetaldehyde complex, 1.1% versus 1.2%, indicates that this effect is due to an interaction along R2 and not the elongation of the H_5−O_2 coordinate. R2 for the HO_2−CH_3CHO is shorter than the analogous R2 for HO−CH_3CHO (3.628 Å). There is no analogous R2 for H_2O−CH_3CHO since water forms a ring with the methyl portion of the acetaldehyde molecule.

Table 2 lists the rotational constants for the hydroperoxyl radical−acetaldehyde complex at all the levels of theory used in this study. At the highest level of theory, B3LYP/6-311++G-(3df,3pd), these constants are 15151, 1802, and 1627 MHz. The molecule is an asymmetric rotor, which is consistent with its structure shown in Figure 5. However, the molecule is also a near-oblate top, as was the hydroxyl radical−acetaldehyde complex. The water−acetaldehyde complex was not a near-oblate top however.

TABLE 10: Geometry of the Hydroperoxyl Radical−Acetaldehyde Complex[a]

	B3LYP			
coordinate	6-31G(d)	6-311++ G(d,p)	6-311++ G(2d,2p)	6-311++ G(3df,3pd)
R1	1.765	1.751	1.741	1.734
R2	2.529	2.740	2.719	2.736
C_1O_1	1.222	1.216	1.215	1.213
C_1H_1	1.105	1.105	1.102	1.103
C_1C_2	1.499	1.495	1.493	1.492
C_2H_2	1.092	1.089	1.087	1.087
C_2H_3	1.098	1.096	1.093	1.093
C_2H_4	1.098	1.096	1.093	1.093
H_5O_2	0.999	0.994	0.993	0.993
O_2O_3	1.333	1.329	1.330	1.325
$H_1C_1O_1$	119.6	119.4	119.4	119.5
$C_2C_1O_1$	123.4	123.8	123.7	123.8
$H_2C_2C_1$	110.9	111.3	111.3	111.4
$H_3C_2C_1$	109.5	109.2	109.2	109.1
$H_4C_2C_1$	109.5	109.2	109.2	109.1
$H_5O_2O_3$	103.5	104.3	104.0	104.2
$C_1O_1H_5$	113.6	118.9	116.8	117.2
$O_1H_5O_2$	164.2	165.2	167.5	167.7
$H_2C_2C_1O_1$	0.0	0.0	0.0	0.0
$H_3C_2C_1O_1$	−121.8	−122.0	−122.0	−122.1
$H_4C_2C_1O_1$	121.8	122.0	122.0	122.1
$C_2C_1O_1H_5$	180.0	180.0	180.0	180.0
$H_1C_1O_1H_5$	0.0	0.0	0.0	0.0
$C_1O_1H_5O_2$	0.0	0.0	0.0	0.0
$O_1H_5O_2O_3$	0.0	0.0	0.0	0.0

[a] Bond distances are given in Ångstroms, bond angles in degrees.

TABLE 11: Vibrational Frequencies of the Hydroperoxyl Radical−Acetaldehyde Complex[a]

		B3LYP/6-311++G(3df,3pd)		
mode number	mode description	frequency	intensity	shift
1	hydroperoxyl H−O stretch	3274	963.6	−328
2	CH_3CHO sp^3 C−H stretch	3144	5.1	+56
3	CH_3CHO sp^3 C−H stretch	3076	2.3	+1
4	CH_3CHO sp^3 C−H stretch	3026	0.9	+3
5	CH_3CHO sp^2 C−H stretch	2968	23.7	−5
6	CH_3CHO C−O stretch	1775	227.0	−38
7	hydroperoxyl H−O−O bend	1573	66.4	+137
8	CH_3CHO sp^3 torsion	1466	10.8	−3
9	CH_3CHO H−C−H bend	1458	28.8	−3
10	CH_3CHO H−C−O bend	1428	6.6	+6
11	CH_3CHO C−C stretch	1384	33.3	+3
12	hydroperoxyl O−O stretch	1199	17.0	+30
13	CH_3CHO H−C−C bend	1149	0.3	+13
14	CH_3CHO H−C−C bend	1141	30.2	+9
15	CH_3CHO torsion	900	8.4	+14
16	CH_3CHO torsion	794	0.2	+15
17	O_1-H_5 stretch	691	106.8	
18	CH_3CHO torsion	532	36.1	+21
19	$O_1-H_5-O_2$ bend	240	37.8	
20	intermolecular tortorsion	165	2.2	
21	CH_3CHO CH_3 twist	164	0.7	+5
22	$C_1-O_1-H_5$ bend	73	8.5	
23	intermolecular torsion	66	0.6	
24	intermolecular torsion	49	6.5	

[a] Frequencies and shifts are given in cm^{-1}; intensities are given in km mol^{-1}.

The hydroperoxyl radical−acetaldehyde complex has 24 normal vibrational modes. Acetaldehyde has 15 vibrational modes and the hydroperoxyl radical has three vibrational modes and the remaining six vibrational modes are intermolecular modes. These modes, their intensities, and shifts from the parent monomers are listed in Table 11. The most intense and most shifted mode is the O−H stretch of the hydroperoxyl radical (mode number 1). This mode has a calculated red shift of 328 cm^{-1} from isolated CH_3CHO. This is larger than a similar shift seen in the HO−CH_3CHO complex by 148 cm^{-1}. This is also larger than the similar shift in the HO_2-CH_2O complex by 69 cm^{-1}. The increased shift in this mode is evidence of a stronger interaction between HO_2 and CH_3CHO than either HO−CH_3-CHO or HO_2-CH_2O. Just as in those complexes, the C−O stretch of HO_2-CH_3CHO (mode 6) is red-shifted relative to that of the isolated organic molecule. The C−O stretch is red-shifted 38 cm^{-1} in the hydroperoxyl radical−acetaldehyde complex, compared to 16 cm^{-1} in the hydroxyl radical−acetaldehyde complex and 30 cm^{-1} in the hydroperoxyl radical−formaldehyde complex. This is further evidence for a stronger interaction in HO_2-CH_3CHO than in HO−CH_3CHO or HO_2-CH_2O. The shift in this particular mode is also larger in the hydroperoxyl radical−acetaldehyde complex than in the water−acetaldehyde complex (18 cm^{-1}), indicating that the hydrogen bond is stronger in HO_2-CH_3CHO than in H_2O-CH_3CHO as well. The remaining vibrational modes of the hydroperoxyl radical, the H−O−O bend (mode 7) and the O−O stretch (mode 12) are both blue-shifted by 137 and 30 cm^{-1}, respectively, to isolated HO_2. These are both larger than those in HO_2-CH_2O, where the shifts in these respective modes are 119 and 28 cm^{-1}. Interestingly, the CH_3CHO sp^2 C−H stretch (mode 5) is red-shifted by 5 cm^{-1}. This can be compared to the analogous mode in the HO−CH_3CHO, which is blue shifted by 41 cm^{-1}. The blue shift in the latter molecule is due to the change in geometry in the acetaldehyde when complexed. However, because of the proximity of the sp^2 hydrogen of acetaldehyde to the terminal oxygen of the hydroperoxyl radical (R2 = 2.736 Å). This is evidence for a second interaction along the R2 coordinate. Contrary to this, mode 2 (primarily the H_2-C_2 stretch) is shifted by 56 cm^{-1} to the blue in both HO−CH_3CHO and HO_2-CH_3-CHO. The intermolecular H_5-O_1 stretch (mode 17) is calculated to have a vibrational frequency of 691 cm^{-1}. This is higher in energy than the analogous mode in HO−CH_3CHO (595 cm^{-1}), H_2O-CH_3CHO (574 cm^{-1}), and HO_2-CH_2O (658 cm^{-1}), reflecting the shorter intermolecular bond distance of HO_2-CH_3CHO. The most intense bands of the hydroperoxyl radical−acetaldehyde complex are modes 1 (963.6 km mol^{-1}), 6 (227.0 km mol^{-1}) and 17 (106.8 km mol^{-1}). Modes 1 and 6 are also more likely to be detected because of the large shifts in these modes relative to isolated acetaldehyde.

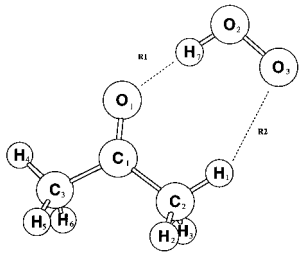

Figure 6. The hydroperoxyl radical−acetone complex.

F. Hydroperoxyl Radical−Acetone Complex. Like acetaldehyde, acetone is not known to react rapidly with the hydroperoxyl radical. However, the possibility of the formation of an adduct via the reaction below has not been adequately addressed.

$$HO_2 + CH_3COCH_3 \rightarrow HO_2-CH_3COCH_3 \qquad (9)$$

In the case of the hydroxyl radical complexes mentioned, as well as the water complexes previously studied,[26] the complexes with acetone were stronger than those with either acetaldehyde or formaldehyde. In this section, we will discuss the properties of $HO_2-CH_3COCH_3$.

The structure of the hydroperoxyl radical−acetone complex is shown in Figure 6. It has a seven-membered structure formed by the HO_2 molecule and the O_1, C_1, C_2, and H_1 atoms of acetone. The fully optimized geometry for $HO_2-CH_3COCH_3$ at all levels of theory used in this study is shown in Table 12. Like the other complexes studied in this work, the primary intermolecular bond (R1) is between the hydrogen of the HO_2 and the oxygen of CH_3COCH_3. This bond distance for R1 is 1.709 Å at the B3LYP/6-311++G(3df,3pd) level of theory. This is the shortest intermolecular bond distance of this study, hence the strongest intermolecular bond. It is 1.5% shorter than R1 for HO_2-CH_3CHO and 4.0% shorter than R1 for HO_2-CH_2O. It is also 9.4%. shorter than R1 for the hydroxyl radical−acetone complex, and 11.8% than R1 for the water−acetone complex. The hydrogen−oxygen bond of the HO_2 is elongated to 0.996 Å, an increase of 2.2% to isolated HO_2. This can be compared to 1.8% for HO_2-CH_3CHO and 1.5% for HO_2-CH_2O; as well as 1.1% for HO−CH_3COCH_3 and 1.2% for $H_2O-CH_3COCH_3$. The carbon−oxygen bond of acetone is elongated by 0.8% to 1.219 Å, which is as large an increase in this coordinate as we have seen thus far. These data all indicates that the hydroperoxyl radical−acetone complex has the strongest intermolecular bond of the molecules in this study. The intermolecular bond distance between the terminal oxygen of HO_2 and H_1 of acetone R2 is 2.449 Å. While this is shorter than any of the other R2 distances we examine in this study, we cannot say that this is a stronger interaction because the hydrogen involved is a methyl hydrogen, while in the aldehydes, the R2 involved a different type of

TABLE 12: Geometry of the Hydroperoxyl Radical−Acetone Complex[a]

	B3LYP			
coordinate	6-31G(d)	6-311++ G(d,p)	6-311++ G(2d,2p)	6-311++ G(3df,3pd)
R1	1.746	1.720	1.715	1.709
R2	2.348	2.476	2.450	2.449
C_1O_1	1.226	1.222	1.221	1.219
C_1C_2	1.511	1.508	1.505	1.504
C_1C_3	1.513	1.509	1.507	1.506
C_2H_1	1.093	1.090	1.087	1.087
C_2H_2	1.098	1.095	1.092	1.092
C_2H_3	1.098	1.095	1.092	1.092
C_3H_4	1.091	1.089	1.086	1.086
C_3H_5	1.097	1.095	1.092	1.092
C_3H_6	1.097	1.094	1.092	1.092
H_7O_2	1.001	0.997	0.996	0.996
O_2O_3	1.331	1.327	1.328	1.323
$C_2C_1O_1$	122.3	122.1	122.1	122.1
$C_3C_2O_1$	120.1	120.3	120.3	120.4
$H_1C_2C_1$	110.7	110.9	110.9	110.8
$H_2C_2C_1$	109.9	109.6	109.7	109.7
$H_3C_2C_1$	109.8	110.9	109.6	109.6
$H_4C_2C_1$	110.2	110.4	110.4	110.5
$H_5C_2C_1$	110.1	109.9	109.9	109.9
$H_6C_2C_1$	110.3	110.1	110.1	110.0
$H_7O_2O_3$	104.8	105.3	105.0	105.2
$C_1O_1H_7$	125.1	130.0	127.9	128.0
$O_1H_7O_2$	179.0	176.8	179.3	179.3
$H_1C_2C_1O_1$	−0.6	−0.7	−0.8	−0.8
$H_2C_2C_1O_1$	−122.3	−122.4	−122.6	−122.7
$H_3C_2C_1O_1$	120.8	120.9	120.7	120.7
$H_4C_3C_1O_1$	−0.8	−0.9	−0.9	−0.9
$H_5C_3C_1O_1$	120.3	120.3	120.4	120.4
$H_6C_3C_1O_1$	−122.2	−122.4	−122.4	−122.4
$C_2C_1O_1H_7$	−0.3	−0.2	−0.2	−0.1
$C_3C_1O_1H_7$	179.7	179.8	179.8	179.9
$C_1O_1H_7O_2$	−19.9	−18.5	−19.1	−18.6
$O_1H_7O_2O_3$	20.7	19.4	19.9	19.4

[a] Bond distances are given in Ångstroms, bond angles in degrees.

hydrogen atom. It can be seen, however, that $C_2-C_1-O_1 \neq C_3-C_1-O_1$ and $H_1-C_2-C_1 \neq H_4-C_3-C_1$. This leads us to believe that some type of interaction exists. Furthermore, the $H_7-O_2-O_3$ bond angle on the hydroperoxyl radical is 105.2° slightly shorter than that in isolated HO_2. This is only a small fraction of a change compared to the same change in HO_2-CH_3CHO (1.1%) and HO_2-CH_2O (1.2%), which leads us to believe that the interaction along R2 is weakest in $HO_2-CH_3COCH_3$.

The rotational constants for the hydroperoxyl radical−acetone complex are given in Table 2. At the B3LYP/6-311++G(3df,3pd) level of theory, these values are 7363, 1493, and 1260 MHz. This is consistent with the structure of $HO_2-CH_3COCH_3$, which is shown in Figure 6. $HO_2-CH_3COCH_3$ is an asymmetric rotor, as are $HO-CH_3COCH_3$ and $H_2O-CH_3COCH_3$.

The hydroperoxyl radical−acetone complex has 33 fundamental modes. Of these, 24 are similar to modes in isolated acetone, three are similar to modes in isolated HO_2, and six are intermolecular modes unique to the complex. These modes are listed in Table 13. As is the case for all the complexes in this study, the most shifted mode is the O−H stretch of the HO_x (HO_2 in this case). That mode (mode number 1) has a calculated red shift of 358 cm^{-1}, the largest of any of the complexes studied in this work. This is evidence that $HO_2-CH_3COCH_3$ is the strongest bound complex studied here. The C−O stretch of acetone (mode 8) is also red-shifted by 36 cm^{-1}, which is also larger than the analogous shifts in the C−O stretching mode of the other complexes, supporting this. This mode has a calculated

TABLE 13: Vibrational Frequencies of the Hydroperoxyl Radical−Acetone Complex[a]

		B3LYP/6-311++G(2d,2p)		
mode number	mode description	frequency	intensity	shift
1	hydroperoxyl H−O stretch	3244	1180.6	−358
2	CH_3COCH_3 C−H stretch	3151	5.7	+5
3	CH_3COCH_3 C−H stretch	3138	1.9	−7
4	CH_3COCH_3 C−H stretch	3094	6.2	+4
5	CH_3COCH_3 C−H stretch	3084	6.2	+2
6	CH_3COCH_3 C−H stretch	3042	5.4	+2
7	CH_3COCH_3 C−H stretch	3032	3.9	0
8	CH_3COCH_3 C−O stretch	1743	271.4	−36
9	hydroperoxyl H−O−O bend	1586	44.4	+150
10	CH_3COCH_3 C−C−H bend	1497	19.1	+4
11	CH_3COCH_3 C−C−H bend	1477	31.0	+1
12	CH_3COCH_3 C−C−H bend	1472	0.9	+2
13	CH_3COCH_3 C−C−H bend	1466	5.4	0
14	CH_3COCH_3 C−C−H bend	1407	43.1	+14
15	CH_3COCH_3 C−C−H bend	1400	38.8	+8
16	CH_3COCH_3 C−C−C asymmetric stretch	1262	61.3	+26
17	hydroperoxyl O−O stretch	1201	15.0	+32
18	CH_3COCH_3 torsion	1130	3.8	+8
19	CH_3COCH_3 C−C−C symmetric stretch	1101	0.4	+11
20	CH_3COCH_3 C−C−O bend	910	5.5	+20
21	CH_3COCH_3 C−C−O bend	898	0.3	+10
22	CH_3COCH_3 torsion	800	0.5	−8
23	H_7-O_1 stretch	713	108.9	
24	CH_3COCH_3 torsion	560	20.7	+24
25	CH_3COCH_3 torsion	498	0.0	+5
26	CH_3COCH_3 torsion	398	9.1	+18
27	$O_1-H_7-O_2$ bend	230	35.1	
28	intermolecular torsion	155	1.8	
29	CH_3COCH_3 torsion	142	0.0	+12
30	$C_1-O_1-H_7$ bend	97	4.0	
31	intermolecular torsion	65	0.2	
32	intermolecular torsion	55	1.5	
33	CH_3COCH_3 torsion	13	0.5	−3

[a] Frequencies and shifts are given in cm^{-1}; intensities are given in km mol^{-1}.

shift that is 16 cm^{-1} larger than the corresponding shift in the water−acetone complex. This is evidence that $HO_2-CH_3COCH_3$ is more strongly bound than $H_2O-CH_3COCH_3$. The H−O−O bend of the hydroperoxyl radical (mode 9) and the O−O stretch of that molecule (mode 17) are shifted to the blue by 150 and 32 cm^{-1}, respectively. These are larger in magnitude than those of either HO_2-CH_2O or HO_2-CH_3CHO, reflecting the stronger effect of acetone complexation on these two modes. Similar to the latter of those two complexes, $HO_2-CH_3COCH_3$ has a carbon−hydrogen stretching mode that is red-shifted (by 7 cm^{-1}), unlike its hydroxyl radical complex counterpart. Not surprisingly, this vibrational mode (mode 3) involves mostly motion by the H_1 atom, which seems to be affected by the terminal oxygen of the hydroperoxyl radical. For the hydroperoxyl radical−acetone complex, the most intense, and presumably most easily detectable bands, are modes 1, 8, and 17. These have calculated band intensities of 1180.6, 271.4, and 108.9 km mol^{-1} respectively.

G. Vibrational Frequencies and Intermolecular Bond Distances. Some comparisons can be made involving the complexes in this study, as well as our previous study of the complexes of these organic molecules with water. The first is between the intermolecular O−H stretching frequency and the intermolecular bond distance along this coordinate (R1). This comparison is made in Figure 7. As one would expect, the intermolecular stretching frequency increases as the intermolecular bond distance decreases. In looking at the complexes in this study and our previous work,[26] examining H_2O complexes with these organic molecules some general statements can be

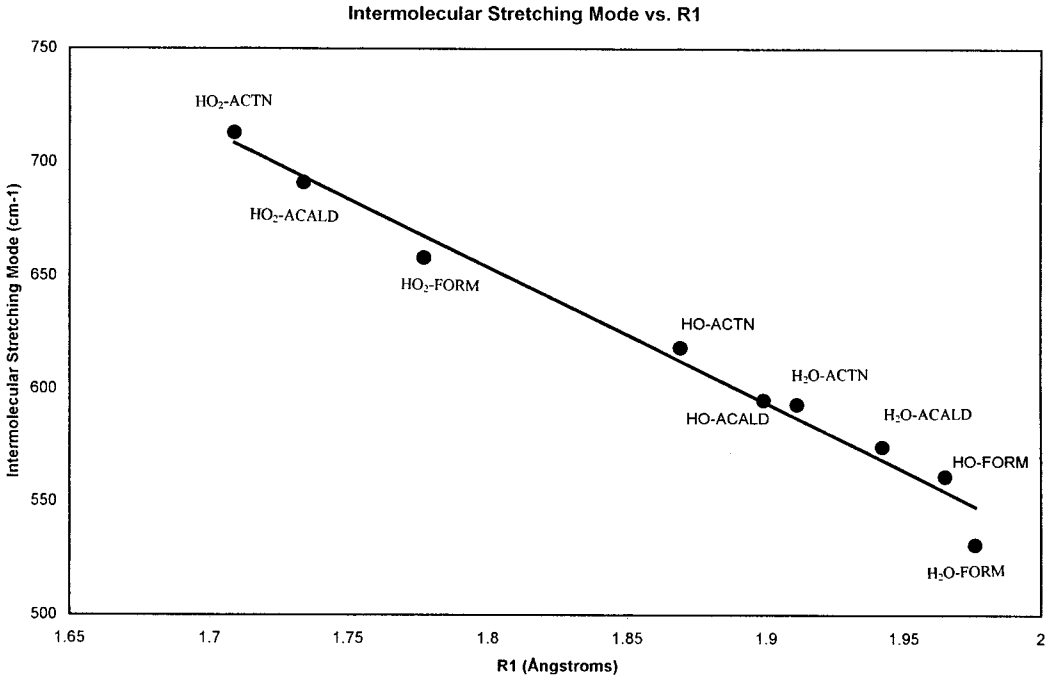

Figure 7. Intermolecular stretching frequency (in cm^{-1}) plotted versus the Intermolecular Bond Distance (R1, in Ångstroms) along the intermolecular bond. Best-fit-line through all the data is included. FORM = formaldehyde, ACALD = acetaldehyde, ACTN = acetone.

made. The data suggest that the identity of the electron acceptor molecule is the most important factor in what the intermolecular bond distance and the intermolecular stretching frequency are. It is clear that complexes involving the hydroperoxyl radical have shorter intermolecular bond distances and larger intermolecular stretching frequencies than those of complexes involving either the hydroxyl radical or water. The acetone and acetaldehyde complexes with the hydroxyl radical have shorter intermolecular bond distances (and larger intermolecular stretching frequencies) than those of any of the water complexes in this study. However, the hydroxyl radical−formaldehyde complex has a longer R1 lower intermolecular stretching frequency than the water−acetone complex or the water−acetaldehyde complex. Within each group of complexes, the general pattern that $R1_{acetone} < R1_{acetaldehyde} < R1_{formaldehyde}$ is seen. Hence, within the hydroperoxyl radical complexes, $HO_2-CH_3COCH_3$ has a shorter R1 than that of HO_2-CH_3CHO, which has a shorter R1 than that of HO_2-CH_2O, and so on. The best-fit-line is given, and has the following equation.

$$\nu_{Ist} = -602\,(R1) + 1736 \qquad (10)$$

In this equation, ν_{Ist} is the intermolecular stretching frequency in cm^{-1}, and R1 is the intermolecular bond distance in Ångstroms. The relationship is fairly linear, with an R^2 value of 0.982. While this equation may be useful when dealing with calculated harmonic frequencies, it may need to be adjusted for predicting intermolecular bond distances due to the anharmonicity of the true potential energy surface.

These types of calculations more accurately predict relative shifts in modes that are similar to isolated monomer modes. We plot the red shift in the O−H stretching frequency of OH, HO_2, and H_2O versus the intermolecular bond distance in Figure 8. Note that water has a asymmetric stretch and a symmetric stretch, of which the former is less affected by complexation than the latter. As one might expect, the shorter the intermolecular bond distance, the more shifted the O−H stretch is in the electron acceptor molecule. As a result of this, the most shifted hydrogen bond frequency involve the complexes of the hydroperoxyl radical. However, this dependence is not clearly linear. It does seem to be linear within each subgroup of complexes involving the same electron acceptor molecule. The shift in the hydroperoxyl O−H stretching mode seems to be more sensitive to changes in the intermolecular bond distance, which is due to different carbonyl-containing molecules as a complexing partner, than any of the shifts of the other O−H stretching modes. The least affected mode is the H−O−H asymmetric stretch of the water complexes.

It would seem that a common vibrational mode to all of the complexes in this study is the carbonyl group C−O stretch. In each of these complexes, this mode is shifted to the red of the similar mode in the isolated parent monomer. This coordinate is of particular importance to the ultraviolet absorption of carbonyl containing molecules because the electrons which are excited in $n \rightarrow \pi^*$ and $\pi \rightarrow \pi^*$ transitions are localized around these atoms. A plot of the shift in the C−O stretch of the carbonyl containing molecule versus the intermolecular bond distance is given in Figure 9. Again, it seems that the identity of the electron acceptor is the most important factor in determining the magnitude of this shift. An interesting observation upon examination of these data is the larger effect on this mode when water is the electron acceptor than the hydroxyl radical. Although the intermolecular bond distance is shorter in the case of the hydroxyl radical−organic species when compared to the corresponding water−organic molecule, the C−O stretch is more affected in each case by H_2O than by OH. This can be somewhat explained when examining the intermolecular C−O−H bond angles for these molecules. The water complexes have smaller C−O−H angles than those of the hydroxyl radical complexes. This sharper angle between the C−O and the intermolecular bond R1 allows the C−O stretch to be less coupled to the R1 coordinate, resulting in a larger red shift in this coordinate. The water complexes, the HO_2-CH_2O complex, and the HO_2-CH_3CHO complex all have similar C−O−H bond angles, and this is reflected in the linearity of their red shifts with respect to intermolecular bond distance. An interesting anomaly is that, in the hydroperoxyl radical−

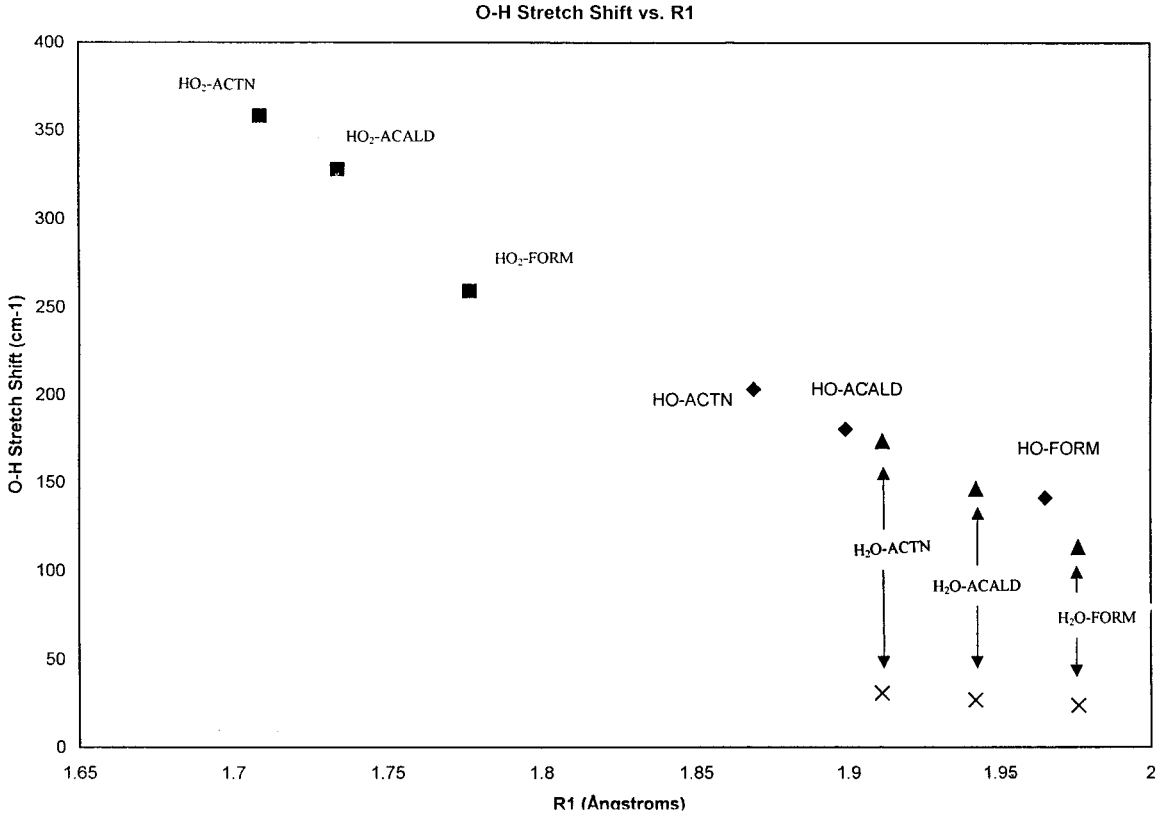

Figure 8. Red shift (in cm^{-1}) of the O−H stretching mode of OH (♦), HO_2 (■), and H_2O (asymmetric shift, ×; asymmetric shift, ▲; versus the intermolecular bond distance (R1, in ångstroms). FORM = formaldehyde, ACALD = acetaldehyde, ACTN = acetone.

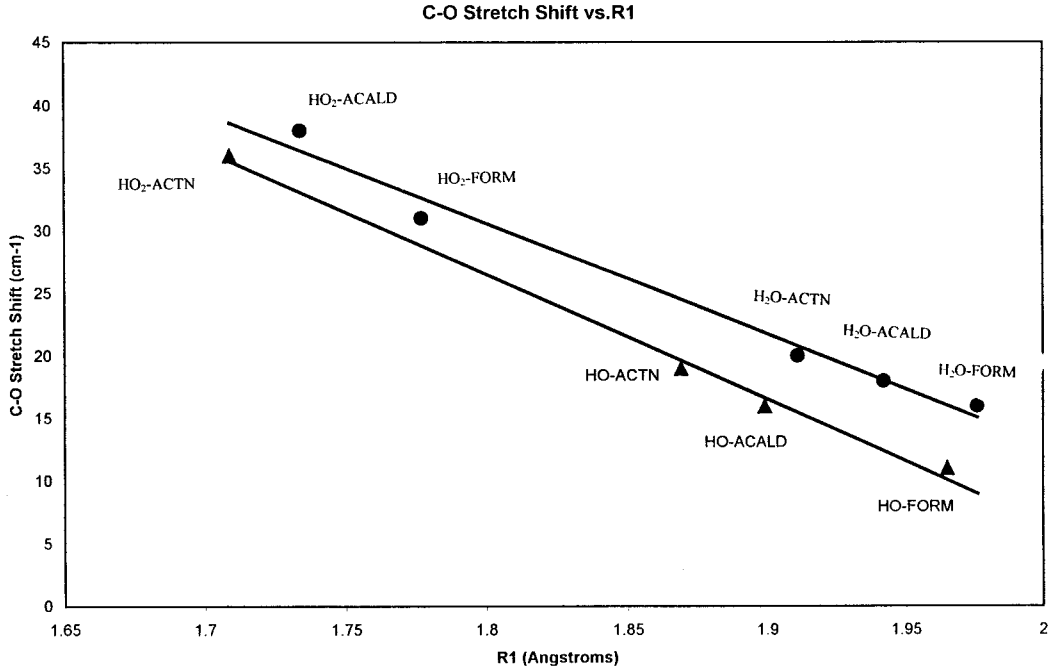

Figure 9. Red shift (in cm^{-1}) of the C−O stretching mode of the organic molecule versus intermolecular bond distances (R1, in Ångstroms). Regression lines included for two data sets based on differing intermolecular C−O−H angles. FORM = formaldehyde, ACALD = acetaldehyde, ACTN = acetone.

carbonyl compound series, the shift in $HO_2-CH_3COCH_3$ is slightly smaller than in HO_2-CH_3CHO, despite the shorter intermolecular bond distance in the former complex. This is reflected in the C−O−H bond angle, for which the hydroperoxyl radical−acetone complex is closer to the hydroxyl radical complexes, whereas the other two hydroperoxyl radical complexes are more similar to the water complexes.

H.The Energetics of the Complexes. The binding energies for the complexes examined in this study are listed in Table 14. The calculated binding energies are listed for all the levels of theory that were used in this work. For each complex, a binding energy is reported with D_o and without the zero-point-energy correction D_e. For all the complexes, the 6-31G(d) basis set overestimates the binding energy when compared to

TABLE 14: Binding Energies of the Complexes[a]

	$HO-CH_2O$		$HO-CH_3CHO$		$HO-CH_3COCH_3$		HO_2-CH_2O		HO_2-CH_3CHO		$HO_2-CH_3COCH_3$	
B3LYP basis set	D_e	D_o	D_e	D_o	D_e	D_o	D_e	D_o	D_e	D_o	D_e	D_o
6-31G(d)	6.2	4.2	7.1	5.3	9.7	7.5	10.8	8.5	12.0	10.0	13.4	11.4
6-311++G(d,p)	5.0	3.3	6.0	4.3	6.6	4.9	8.5	6.5	9.8	8.1	11.0	9.2
6-311++G(2d,2p)	4.8	3.0	5.7	4.0	6.4	4.6	8.3	6.3	9.6	7.8	10.6	8.8
6-311++G(3df,3pd)	4.9	3.0	5.8	4.0	6.4	4.6	8.4	6.3	9.6	7.8	10.7	8.9

[a] All binding energies are reported in kcal mol^{-1}.

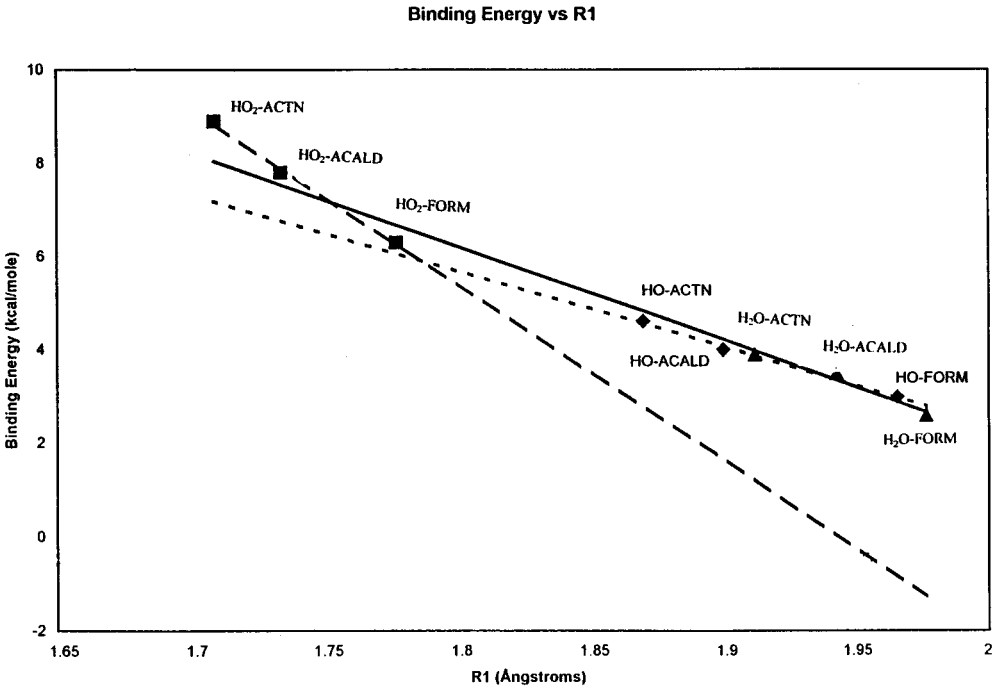

Figure 10. Binding energy of the complex (in kcal mol^{-1}) versus the intermolecular bond distance (R1, in Ångstroms). Best-fit-line included for complexes involving H_2O (solid), OH (dotted), and HO_2 (dashed). FORM = formaldehyde, ACALD = acetaldehyde, ACTN = acetone.

the larger basis sets. This error ranges from 22% in the case of the D_e for the hydroxyl radical−acetaldehyde complex, to 63% in the case of the D_o for the hydroxyl radical−acetone complex. It is clear that larger basis sets need to be used in order to predict binding energies of complexes more accurately.

The identity of the organic hydrogen acceptor molecule has an effect on the binding energy that shows a clear pattern. From the data, it can be seen that acetone forms the most strongly bound complexes and formaldehyde makes the weakest bound ones. This is the same trend that is seen in the analogous water complexes.[26] For the hydroxyl radical complexes, the binding energies D_o are 3.0, 4.0, and 4.6 kcal mol^{-1} at the B3LYP/6-311++G(3df,3pd) for formaldehyde, acetaldehyde, and acetone, respectively. This amounts to an increase in the binding energy of 29% from $HO-CH_2O$ to $HO-CH_3CHO$ and 14% from $HO-CH_3CHO$ to $HO-CH_3COCH_3$. The binding energies D_o for the hydroperoxyl radical complexes at the same level of theory are 6.3, 7.8 and 8.9 kcal mol^{-1} for formaldehyde, acetaldehyde, and acetone, respectively. This is a 22% increase from HO_2-CH_2O to HO_2-CH_3CHO, and a 13% increase from HO_2-CH_3CHO to $HO_2-CH_3COCH_3$. At the same level of theory, water−formaldehyde has a binding energy D_o of 2.6 kcal mol^{-1}, water−acetaldehyde has a binding energy of 3.5 kcal mol^{-1}, and water−acetone has a binding energy of 3.9 kcal mol^{-1}. This follows a similar pattern, with increases in binding energy of 30% and 11% for each of the complexes.

The identity of the hydrogen donor molecule also follows a pattern in terms of the binding energy of the complexes. The hydroperoxyl radical forms complexes that are more strongly bound than either the complexes formed by the hydroxyl radical or the complexes formed by water. The HO_2-CH_2O complex has a binding energy that is 3.3 kcal mol^{-1} larger than that of $HO-CH_2O$ and 3.7 kcal mol^{-1} larger than that of H_2O-CH_2O. The same general trend in increased binding energy can be seen in the other carbonyl complexes. In each case, complexes with HO_2 as the hydrogen donor have binding energies that are around double that of ones with HO or H_2O.

One of the things that these much stronger binding energies can be attributed to, is a stronger hydrogen bond along the R1 coordinate. Figure 10 shows the relationship between binding energy and intermolecular bond distance along this coordinate. Included are best-fit-lines for each subset of hydrogen donor molecule. It is clear that in every case, as one would expect, the shorter the bond distance, the more strongly bound the complex. This effect is stronger with the more strongly bound complexes of HO_2, as the slope of the line indicates. A second reason as to why HO_2 forms more strongly bound complexes is the interaction between the terminal oxygen in the hydroperoxyl radical, and one of the hydrogen atoms of the carbonyl containing molecule. The evidence from the data above involving differences in structure and vibrational frequencies in the coordinates nearest to this terminal oxygen supports that such an interaction exists and contributes to the binding energy. As can be seen in the geometry tables, the R2 coordinate is much shorter for the HO_2 complexes than for the OH complexes. For the carbonyls we studied, this difference was as small as 0.523 Å in the acetone complexes, and as large as 1.002 Å in the formaldehyde complexes.

TABLE 15: Thermodynamic Properties of the Complexes[a]

species	ΔH_f^0	ΔH_f^{200}	ΔH_f^{300}	ΔS^{200}	ΔS^{300}	K_f^{200}	K_f^{300}
OH	9.3	9.3	9.3	41.9	43.9		
HO_2	3.5	3.0	2.8	51.9	54.4		
CH_2O	−23.9	−24.6	−26.0	49.7	52.3		
CH_3CHO	−35.5	−36.9	−39.7	58.7	63.2		
CH_3COCH_3	−45.8	−47.8	−51.9	63.7	70.5		
$HO-CH_2O$	−17.6	−19.5	−20.4	67.4	73.3	4.2×10^{-21}	2.0×10^{-22}
$HO-CH_3CHO$	−30.2	−33.5	−35.1	73.9	81.7	1.1×10^{-19}	3.0×10^{-22}
$HO-CH_3COCH_3$	−41.1	−45.7	−47.9	82.8	92.9	1.7×10^{-17}	6.3×10^{-21}
HO_2-CH_2O	−26.7	−28.1	−28.8	72.3	79.2	1.4×10^{-19}	4.8×10^{-22}
HO_2-CH_3CHO	−39.8	−42.6	−44.0	79.3	88.2	1.5×10^{-17}	2.3×10^{-21}
$HO_2-CH_3COCH_3$	−51.3	−55.3	−57.4	87.8	98.8	7.0×10^{-15}	8.5×10^{-20}

[a] Enthalpies are reported in kcal mol^{-1}, entropies in cal mol^{-1} K^{-1}, and equilibrium constants in cm^3 $molecule^{-1}$.

Hydroxyl radical forms stronger complexes with carbonyl groups than water. The OH complexes with CH_2O, CH_3CHO, and CH_3COCH_3 are 0.4, 0.5, and 0.7 kcal mol^{-1} stronger than their corresponding H_2O complexes. In a previous study of the H_2O-CH_2O complex, Ramelot et al.[22] report that there is no interaction between the oxygen atom of the water and the nearest hydrogen atom of the formaldehyde. However, when we notice that while the H−C bond distances remain equal in the water−formaldehyde complex, the H−C−O angles are slightly different, indicating that an small interaction may exist. The calculated R2 value for H_2O-CH_2O is 2.909 Å. For H_2O-CH_3CHO and $H_2O-CH_3COCH_3$, R2 is 2.588 and 2.598 Å, respectively. In the former case, this is a shorter distance than that for HO_2-CH_3CHO. It would seem that an interaction would exist along this coordinate which would increase the binding energy of the water complex with respect to that of the hydroxyl radical complexes, for which this interaction would be much weaker. However, the strength of the hydroxyl radical complexes' bond along the R1 coordinate is stronger than the corresponding bonds along the same coordinate in the water complexes by at least the difference in their binding energies, and perhaps more. This difference reflects the greater stabilization of the open shell system by complexation, when compared to the closed shell system.

Using the data from our calculations, it is possible to calculate relevant thermodynamic properties of the formation of these complexes. These data, along with the values used for the parent monomers, is listed in Table 15. Room-temperature data for the monomers was taken from NASA's JPL Publication 97-4.[31] These data were extrapolated to other temperatures using Kirchhoff's Law:

$$\Delta H(T_2) - \Delta H(T_1) = \Delta C_p \, \Delta T \qquad (11)$$

where T is the temperature and ΔC_p is the difference in heat capacity at constant pressure of the substances whose enthalpy is being calculated to those of the elements in their natural state. Differences in heat capacities were assumed to be independent of temperature. Entropies were extrapolated to different temperatures using the following equation:

$$S(T_2) - S(T_1) = C_v \ln(T_2/T_1) \qquad (12)$$

where C_v is the heat capacity at constant volume. The enthalpies of formation ΔH_f and entropies S have been calculated for the complexes at 200 and at 300 K.

We can use these data to calculate the equilibrium constant for the formation of each complex from its parent monomers. These data are also listed in Table 15. While these equilibrium constants are quite low at room temperature, at lower temperatures some of them are predicted to rise dramatically. The equilibrium constant for the hydroperoxyl radical−acetone complex rises nearly 5 orders of magnitude when calculated from 300 to 200 K. At 200 K, the equilibrium constant is 7.0×10^{-15} cm^3 $molecule^{-1}$, while at 300 K this value is 8.5×10^{-20}. To put this into perspective, the equilibrium constant for the formation of the N_2O_4 dimer from NO_2 is 2.5×10^{-19} cm^3 $molecule^{-1}$ at 298 K and 1.4×10^{-14} at 200 K.[31] This means the formation of $HO_2-CH_3COCH_3$ may be possible under some atmospheric conditions. Recent measurements in the upper troposphere of acetone estimate a number density of 2×10^{10} molecule cm^{-3}. If the temperature is 200 K and the HO_2 number density is 5×10^8 molecules cm^{-3}, then the equilibrium concentration of $HO_2-CH_3COCH_3$ would be 7×10^5 molecules cm^{-3}. This is a small percentage of the concentration of the parent monomers whose effect on the chemistry of the atmosphere is not clear.

IV. Conclusions

In this work, we have calculated the structure and energetics of complexes involving the hydroxyl and hydroperoxyl radical and the carbonyl containing molecules formaldehyde, acetaldehyde and acetone. These open shell complexes are more strongly bound than are their corresponding closed shell water counterparts. The hydroperoxyl radical complexes have significantly larger binding energies than either the hydroxyl radical complexes or the water complexes. Within each subgroup of hydrogen donor complex, acetone forms the strongest complexes and formaldehyde forms the weakest. Furthermore, acetone and acetaldehyde are not known to react quickly with the hydroperoxyl radical. For this reason, it is most likely that these complexes may be detectable.

Acknowledgment. The authors thank Dr. Sabre Kais and Stephan Belair, as well as the other members of our research group, for useful discussions regarding the scientific content of this work.

References and Notes

(1) Li, J. C.; Ross, D. K. *Nature* **1993**, *365*, 327.
(2) For a review of studies of $(H_2O)_n$ complexes, see: Scheiner, S. *Annu. Rev. Phys. Chem.* **1994**, *45*, 23.
(3) Rybak, S.; Jeziorski, B.; Szalewicz, K. *J. Chem. Phys.* **1991**, *95*, 6576.
(4) Feller, D. *J. Chem. Phys.* **1992**, *96*, 6104.
(5) Kim, K. S.; Mhin, B. J.; Choi, U.; Lee, K. *J. Chem. Phys.* **1992**, 6649.
(6) Xantheas, S. S.; Dunning, T. H. *J. Chem. Phys.* **1993**, *99*, 8774.
(7) Chakravorty, S. J.; Davidson, E. R. *J. Phys. Chem.* **1993**, *97*, 6373.
(8) Feller, D. E.; Glendening, E. D.; Kendall, R. A.; Perterson, K. A. *J. Chem. Phys.* **1994**, *100*, 4981.
(9) Mok, D. K. W.; Handy, N. C.; Amos, R. *Mol. Phys.* **1997**, *92*, 667.
(10) Schütz, M.; Rauhut, G.; Werner, H.-J. *J. Phys. Chem.* **1998**, *102*, 5997.
(11) Novoa, J. J.; Sosa, C. P. *J. Phys. Chem.* **1995**, *99*, 15837.
(12) Morokuma, K. *J. Chem. Phys.* **1971**, *55*, 1236.
(13) Del Bene, J. E. *J. Am. Chem. Soc.* **1973**, *95*, 6517.
(14) Butler, L. G.; Brown, T. L. *J. Am. Chem. Soc.* **1981**, *103*, 6541.
(15) Williams, I. H.; Spangler, D.; Femec, D. A.; Maggiora, G. M.; Schowen, R. L. *J. Am. Chem. Soc.* **1983**, *105*, 31.
(16) Williams, I. H. *J. Am. Chem. Soc.* **1987**, *109*, 6229.
(17) Blair, J. T.; Westbrook, J. D.; Levy, R. M.; Krogh-Jespersen, K. *Chem. Phys. Lett.* **1989**, *154*, 531.
(18) Kumpf, R. A.; Damewood, J. R. *J. Phys. Chem.* **1989**, *93*, 4478.

(19) Vos, R. J.; Hendriks, R.; van Duijneveldt, F. B. *J. Comput. Chem.* **1990**, *11*, 1.
(20) Zhang, X. K.; Lewars, E. G.; March, R. E.; Parnis, J. K. *J. Phys. Chem.* **1993**, *97*, 4320.
(21) Stefanovich, E. V.; Truong, T. N. *J. Chem. Phys.* **1996**, *105*, 2961.
(22) Ramelot, T. A.; Hu, C. H.; Fowler, J. E.; DeLeeuw, B. J.; Schaefer, H. F., III *J. Chem. Phys.* **1994**, *100*, 4347.
(23) Liao, D.-W.; Mebel, A. M.; Chen, Y.-T.; Lin, S.-H. *J. Phys. Chem.* **1997**, *101*, 9925.
(24) Rablen, P. R.; Lockman, J. W.; Jorgensen, W. L. *J. Phys. Chem.* **1998**, *102*, 3782.
(25) Tsuzuki, S.; Uchimaru, T.; Matsumura, K.; Mikami, M.; Tanabe, K. *J. Chem. Phys.* **1999**, *110*, 11906.
(26) Aloisio, S.; Francisco, J. S. *Phys. Chem. Earth* **1999**. In press.
(27) Nelander, B. *J. Chem. Phys.* **1980**, *72*, 77.
(28) Nelander, B.; *Chem. Phys.* **1992**, *159*, 281.
(29) For a calculation of a binding energy (D_e) of 5.6 kcal mol^{-1}, see: Xie, Y.; Schaefer, H. F., III *J. Chem. Phys.* **1993**, *94*, 2057.
(30) Hamilton, E. J.; Naleway, C. A. *J. Phys. Chem.* **1976**, *80*, 2037 first calculated a structure for HO_2-H_2O. Our recent calculations estimate a binding energy (D_e) of 8.8 kcal mol^{-1}.
(31) DeMore, W. B.; Sander, S. P.; Golden, D. M.; Hampson, R. F.; Kurylo, M. J.; Howard, C. J.; Ravishankara, A. R.; Kolb, C. E.; Molina, M. J. Chemical Kinetics and Photochemical Data for Use in Stratospheric Modelling. Evaluation No. 12; National Aeronautics and Space Administration-Jet Propulsion Laboratory: Pasadena. 1997 and references therein.
(32) Frisch, M. J.; Trucks, G. W.; Schlegel, H. G.; Gill, P. M. W.; Johnson, B. G.; Robb, M. A.; Cheeseman, J. R.; Keith, T.; Petersson, G. A.; Montgomery, J. A.; Raghavachari, K.; Al-Laham, M. A.; Zakrzewski, V. G.; Ortiz, J. V.; Foresman, J. B.; Cioslowski, J.; Stefanov, B. B.; Nanayakkara, A.; Challacombe, M.; Peng, C. Y.; Ayala, P. Y.; Chen, W.; Wong, M. W.; Andres, J. L.; Replogle, E. S.; Gomperts, R.; Martin, R. L.; Fox, D. J.; Binkley, J. S.; Defrees, D. J.; Baker, J.; Stewart, J. P.; Head-Gordon, M.; Gonzalez, C.; Pople, J. A. GAUSSIAN 94, Revision D.2; GAUSSIAN, Inc.: Pittsburgh, PA,1995,
(33) Becke, A. M. *J. Chem. Phys.* **1993**, *98*, 5648.
(34) Latajka, Z.; Bouteiller, Y. *J. Chem. Phys.* **1994**, *101*, 9793.
(35) Kim, K.; Jordan, K. D. *J. Phys. Chem.* **1994**, *98*, 10089.
(36) Del Bene, J. E.; Person, W. B.; Szczepaniak, K. *J. Phys. Chem.* **1995**, *99*, 10705.
(37) Montgomery, J. A., Jr.; Frisch, M. J.; Ochterski, J. W.; Petersson, G. A. *J. Chem. Phys.* **1999**, *110*, 2822.
(38) Horowitz, A.; Su, F.; Calvert, J. G. *Int. J. Chem. Kinet.* **1978**, *10*, 1099.
(39) Niki, H.; Maker, P. D.; Savage, C. M.; Breitenbach, L. P. *J. Phys. Chem.* **1984**, *88*, 2116.
(40) Temps, F.; Wagner, H. G. *Ber. Bunsen-Ges. Phys. Chem.* **1984**, *88*, 415.
(41) Cheung, Y.-S.; Li, W.-K. *Theochem* **1995**, *333*, 135.
(42) Atkinson, R.; Pitts, J. N., Jr. *J. Chem. Phys.* **1978**, *68*, 3851.
(43) Michael, J. V.; Keil, D. G.; Klemm, R. M. *J. Chem. Phys.* **1985**, *83*, 1630.
(44) Semmes, D. H.; Ravishankara, A. R.; Gump-Perkins, C. A.; Wine, P. H. *Int. J. Chem. Kinet.* **1985**, *17*, 303.
(45) Wallington, T. J.; Kurylo, M. J. *J. Phys. Chem.* **1987**, *91*, 5050.
(46) Horner, E. C. A.; Style, D. W. G.; Summers, D. *Trans. Faraday Soc.* **1954**, *50*, 1201.
(47) Su, F.; Calvert, J. G.; Shaw, J. H.; Niki, H.; Maker, P. D.; Savage, C. M.; Breitenbach, L. D. *Chem. Phys. Lett.* **1979**, *65*, 221.
(48) Su, F.; Calvert, J. G.; Shaw, J. H. *J. Phys. Chem.* **1979**, *83*, 3185.
(49) Veyret, B.; Lesclaux, R.; Rayez, M.-T.; Rayez, J.-C.; Cox, R. A.; Moortgat, G. K. *J. Phys. Chem.* **1989**, *93*, 2368.
(50) Finlayson-Pitts, B. J.; Pitts, J. N., Jr. *Atmospheric Chemistry*; Wiley: New York, 1986.